Optics Letters

Phase-only color rainbow holographic near-eye display

Xin Yang,[1] Shuming Jiao,[2,*] Qiang Song,[1] Guo-Bin Ma,[1] and Weiwei Cai[3]

[1]Lochn Micro/Nano Photonics Research Center, Shenzhen 518000, China
[2]Peng Cheng Laboratory, Shenzhen 518055, China
[3]Key Lab of Education Ministry for Power Machinery and Engineering, School of Mechanical Engineering, Shanghai Jiao Tong University, Shanghai 200240, China
*Corresponding author: jiaoshm@pcl.ac.cn

Received 18 May 2021; revised 7 October 2021; accepted 11 October 2021; posted 12 October 2021 (Doc. ID 431769); published 28 October 2021

Color rainbow holography can realize color holographic 3D display without speckle noise under white light illumination. However, traditional color rainbow holograms used for high-resolution static color 3D display or near-eye color display are amplitude-type, resulting in low diffraction efficiency due to the presence of conjugate light. In this Letter, a phase-only color rainbow holographic near-eye display is demonstrated. The calculation of a phase-only color rainbow hologram is realized by combining a band-limited diffraction and a bi-directional error diffusion algorithm with high-frequency blazed gratings coded to control longitudinal dispersion. When the wavelength of illumination light is deviated from the designated wavelength of the hologram, only a certain wavefront aberration is caused, but there is no conjugate light. The phase-only color rainbow holographic near-eye display of both a 2D color image and a 3D scene are implemented by optical experiments. It has potential applications in head-mounted 3D augmented reality displays without vergence-accommodation conflict.

https://doi.org/10.1364/OL.431769

Holographic near-eye display is regarded as the next generation optics for augmented reality (AR) or virtual reality (VR) displays due to its capability of fully reconstructing a complex-amplitude diffracted light field from a 3D scene [1]. It is a very critical feature that holographic near-eye display is free of vergence-accommodation conflict (VAC), which causes viewers' fatigue and discomfort when compared with conventional stereoscopic 3D display. Alternative techniques such as varifocal near-eye displays [2], multi-layer near-eye displays [3], and light field near-eye displays [4] can also weaken the VAC but would bring some limitations. A variety of holographic near-eye displays have been proposed. For example, in 2017, a holographic near-eye 3D display based on an off-axis volume holographic lens was realized, providing a field of view of 80° [5]. Double-phase holograms were used for display with laser illumination. In order to extend the eye-box size, optical combiners by spatial multiplexing have been demonstrated [6,7]. A holographic near-eye device has also been demonstrated in [8] by displaying 3D light-field holographic images with a large field of view using spherical wave illumination. The holographic near-eye grayscale or color 3D displays with a compact form factor have also been demonstrated by spatial division of the spatial light modulator (SLM) and beam combining with grating to achieve complex-amplitude modulation [9,10]. Despite successful demonstrations, these techniques all use lasers as its light source, which results in unavoidable speckle noise that is challenging to handle.

Rainbow holography, a very classic holographic color 3D display technique, can effectively overcome the aforementioned limitation by using incoherent white light illumination [11,12]. The traditional rainbow holography, however, is either realized by optical exposure [11] or by micro-nano output of high-resolution computer-generated holograms [12] for static color 3D display. Recently, the Fourier rainbow holography has been proposed for near-eye display by using a grating to disperse the white light in the longitudinal direction. Then the dispersed light illuminates the SLM for dynamic 3D display [13]. However, this method can only achieve a rainbow color changing display instead of a full-color display. A full-color dynamic rainbow holographic near-eye 3D display using the 4K LCoS (liquid crystal on silicon) has been proposed in [14]. However, the amplitude hologram suffers from low diffraction efficiency due to the conjugate light pattern [15,16].

Various methods can be used to calculate a phase-only hologram, such as the Gerchberg–Saxton (GS) algorithm and its variants [17], the double-phase method [18] and the error diffusion algorithm [19–21]. However, the iterative GS algorithm is computationally inefficient, and the double-phase holography reduces the spatial resolution and leads to more complex spectral components. In our work, a tailor-made bi-directional error diffusion algorithm is adopted to optimize the phase distribution on the holographic plane for high-fidelity object image reconstruction [19].

In this Letter, the calculation steps of a phase-only color rainbow hologram are demonstrated. The complex-amplitude distributions of diffracted object light fields on the holographic plane in three primary color channels are first calculated according to the band-limited angular spectrum diffraction. Then the three corresponding optimized phase distributions are obtained

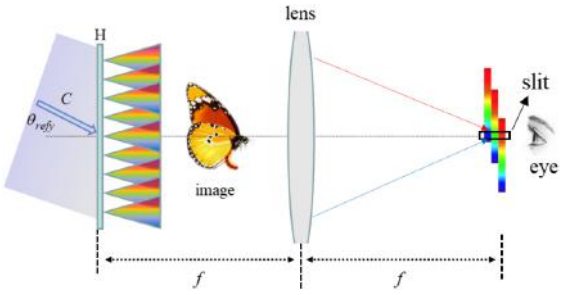

Fig. 1. Illustration of optical system for phase-only color rainbow holographic near-eye display.

by a bi-directional error diffusion algorithm, and the phases of reference light corresponding to each color are coded separately to form three phase-only rainbow sub-holograms for each color. The three phase-only sub-holograms are superimposed to obtain the phase-only color rainbow hologram. A compact display system comprising a white light source, a collimating lens, a beam splitter, a phase-only LCoS, a $4f$ optical filtering system, and an eyepiece is established to experimentally demonstrate a 2D/3D color holographic near-eye display.

Figure 1 shows the optical system for a phase-only color rainbow holographic near-eye display. The plane-wave white light C illuminates the phase-only rainbow hologram H with an off-axis angle of θ_{refy}. The hologram H is located at the front focal plane of the lens. After the diffracted light from the hologram propagates by a certain distance, the reconstructed image is formed with longitudinal dispersion. On the back focal plane of the lens, three sets of longitudinal misaligned superimposed spectral distributions are formed. When the human eye is at the slit, the narrow bands of red, green, and blue spectra enter the human eye at the same time, and an accurate color reproduction image can be seen. When the human eye moves longitudinally, the effect of the rainbow color change can be perceived. Different from the amplitude color rainbow hologram [14], the phase-only color rainbow hologram theoretically only forms the first-order diffracted light after diffraction, which can be expressed as

$$H = \sum_{c=r,g,b} \exp\left\{ i\left[\varphi_{oc} - \frac{2\pi}{\lambda_c} y \sin\left(\theta_{\text{refy}}\right)\right]\right\}, \tag{1}$$

where $c = r, g, b$ represents the three primary colors, i.e., red, green, and blue. φ_{oc} represents the three phase distributions of the object light on the holographic plane under the band-limited condition, and $\frac{2\pi}{\lambda_c} y \sin(\theta_{\text{refy}})$ represents the phase of reference waves of the three primary colors. Equation (1) suggests that the phase-only color rainbow hologram is formed by superimposing three phase-only sub-holograms in three color channels.

In the hologram reconstruction, the illuminating plane wave C can be expressed as

$$C = \exp\left[i \frac{2\pi}{\lambda'} y \sin\left(\theta_{\text{refy}}\right)\right], \tag{2}$$

where λ' represents the wavelength covered by the white light source.

The diffracted light behind the hologram can be expressed as

$$U = HC = \sum_{c=r,g,b} \exp\left\{ i\left[\varphi_{oc} + 2\pi y \sin(\theta_{\text{refy}}) \left(\frac{1}{\lambda'} - \frac{1}{\lambda_c}\right)\right]\right\}. \tag{3}$$

When the wavelength of illuminating light is the same as the recording light of the three primary colors, $\exp[i\varphi_{or}]$, $\exp[i\varphi_{og}]$, and $\exp[i\varphi_{ob}]$ can be obtained. Otherwise, three sets of carrier frequencies are formed

$$f_{rc} = \left(\frac{1}{\lambda'} - \frac{1}{\lambda_c}\right) \sin\left(\theta_{\text{refy}}\right) = \frac{\sin(\theta')}{\lambda'}. \tag{4}$$

Consequently, a longitudinal dispersion for three sets of spectra can be generated, and θ' is the diffraction angle corresponding to each wavelength λ'. It can be inferred that the spectral expansion causes wavefront phase difference instead of high-order diffracted light. This yields dispersion in the reproduced image at the original recording position, and the slit can be used to extract the local spectral components. Consequently, the fidelity of the dispersed image seen by the human eye can be guaranteed.

Therefore, under the band-limited condition, optimizing three-color phase distributions and then encoding the phases of the corresponding reference lights are the most critical steps for the calculation of the phase-only color rainbow hologram.

The calculation methods of the phase-only color rainbow holograms of the 2D color image and the 3D color object are described as follows:

The phase-only color rainbow hologram calculation of the 2D image denotes I as the target color image and H as the holographic plane. According to the angular spectrum diffraction theory, the complex-amplitude diffracted object light with band-limited condition can be calculated as

$$U_c = \Im^{-1}\left[\Im(I_c) \times H_c(f_x, f_y) \times F(f_x, f_y)\right], \tag{5}$$

where $I_c(c = r, g, b)$ represents the color channels of the target color image. $\Im$ and $\Im^{-1}$ represent the 2D Fourier transform and the inverse Fourier transform. The optical transfer function is $H_c(f_x, f_y) = \exp\left[i \frac{2\pi}{\lambda_c} z \sqrt{1 - (\lambda_c f_x)^2 - (\lambda_c f_y)^2}\right]$, and F is a slit-type binary filter that can be expressed as

$$F(f_x, f_y) = \begin{cases} 1 & |f_y| < f_{yb} \\ 0 & \text{else} \end{cases}, \tag{6}$$

where f_{yb} is the maximum frequency in the longitudinal direction, and the bandwidth of the object wave on the hologram plane is $2 f_{yb}$.

After three complex-amplitude distributions, U_r, U_g, and U_b are calculated, and the optimized phase distribution for each color can be expressed as

$$\varphi_c = \Gamma\{\mathrm{U_c}\}, \tag{7}$$

where Γ denotes the tailor-made bi-directional error diffusion algorithm. In this study, the pixel scanning direction is optimized vertically rather than horizontally. As shown in Fig. 2(a), each square represents a pixel with a coordinate of (x, y). The scanning starts from the first pixel in the upper left corner, and the ping-pong scanning method is applied to each odd/even column of pixels with alternating scanning directions.

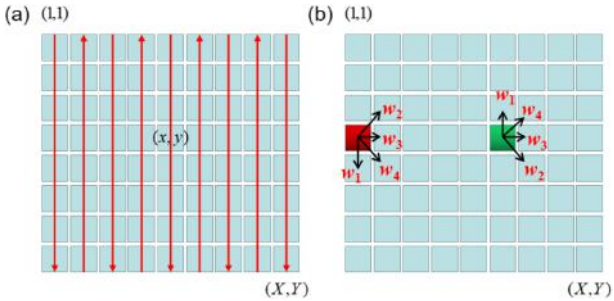

Fig. 2. Tailor-made bi-directional error diffusion algorithm for phase full-color rainbow hologram calculation.

The original complex-amplitude distribution $U_c(x, y)$ can be expressed as

$$U_c(x, y) = A_c \exp[i\varphi_{oc}(x, y)]. \tag{8}$$

Only the phase component is preserved, and the error can be expressed as

$$E(x, y) = U_c(x, y) - \exp[i\varphi_{oc}(x, y)]. \tag{9}$$

The error spreads to adjacent pixels with predefined weighting factors. As shown in Fig. 2(b), a red pixel represents the pixel located in an odd column, and the error spreads to the vicinity in the following way

$$\begin{aligned} U_c(x, y+1) &\leftarrow U_c(x, y+1) + w_1 E(x, y) \\ U_c(x-1, y-1) &\leftarrow U_c(x-1, y-1) + w_2 E(x, y) \\ U_c(x+1, y) &\leftarrow U_c(x+1, y) + w_3 E(x, y) \\ U_c(x+1, y+1) &\leftarrow U_c(x+1, y+1) + w_4 E(x, y). \end{aligned} \tag{10}$$

For each pixel in the even column, like the green pixel in Fig. 2(b), the error spreads in the following way

$$\begin{aligned} U_c(x-1, y) &\leftarrow U_c(x-1, y) + w_1 E(x, y) \\ U_c(x+1, y+1) &\leftarrow U_c(x+1, y+1) + w_2 E(x, y) \\ U_c(x, y+1) &\leftarrow U_c(x, y+1) + w_3 E(x, y) \\ U_c(x-1, y+1) &\leftarrow U_c(x-1, y+1) + w_4 E(x, y), \end{aligned} \tag{11}$$

where $w_1 = 7/16$, $w_2 = 3/16$, $w_3 = 5/16$, and $w_4 = 1/16$ are always used in the calculation. The phase distributions φ_{or}, φ_{og}, and φ_{ob} for the three colors can be independently optimized in this manner.

In the phase-only color rainbow hologram calculation of the 3D image, the 3D color object used for phase-only color rainbow hologram calculation is represented by a RGB-D model. For example, Fig. 3(a) is a RGB color image, and Fig. 3(b) is the corresponding depth map. The complex-amplitude hologram of a 3D color object can be calculated by layered diffraction, which can be expressed as

$$U_c = \sum_{z=z_{\min}:z_{\max}} \Im^{-1}\left[\Im(I_{cz}) \times H(f_x, f_y, z) \times F(f_x, f_y)\right], \tag{12}$$

where $z_{\min}$ and $z_{\max}$ are the closest and furthest distances between the 3D image and the hologram plane, respectively. I_{cz} is the color intensity distribution of the c-channel image for each distance z. $F(f_x, f_y)$ is a slit-type binary filter that is the same as in Eq. (6).

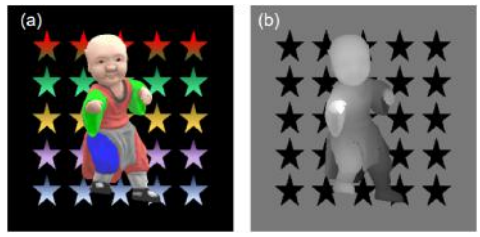

Fig. 3. 3D object model for the phase-only color rainbow hologram calculation: (a) RGB color image and (b) depth map.

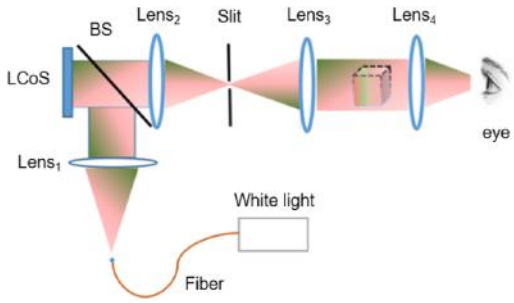

Fig. 4. Experimental setup for the color holographic near-eye display.

The optimized phase distributions φ_r, φ_g, and φ_b can be further calculated by Eq. (7), and then the phase-only color rainbow hologram can be calculated by Eq. (1) for near-eye display.

The experimental setup for color holographic near-eye display is demonstrated in Fig. 4. After the divergent light from the fiber tip is collimated by Lens_1, it is partially reflected by the beam-splitter to illuminate the phase-only LCoS with a resolution of 3840×2160 pixels and a pixel pitch of $3.74\ \mu\text{m}\,f$. At the same time, the phase-only color rainbow hologram is loaded to modulate the illumination light. The diffracted wave is filtered by a $4f$ optical system including Lens_2 and Lens_3 with a slit filter. A real reconstructed color image is formed at a distance from Lens_3, and the enlarged image can be viewed by the human eye with the eyepiece in Lens_4.

A Beijing Opera facial makeup image with a resolution of 2000×2000 pixels was used for the calculation of the phase-only color rainbow hologram, as shown in Fig. 5(a). The distance between the 2D color image and the hologram plane is 5 mm, and the primary wavelengths are 467 nm, 532 nm, and 632 nm, respectively. The reference wave has an illumination angle $\theta_{\text{refy}} = 3°$. The bandwidth was set to be 20 lp/mm in the hologram calculation. Figure 5(b) is the calculated phase-only color rainbow hologram, and Fig. 5(d) is the numerically reconstructed image. The experimental full-color display results can be successfully obtained, shown in Figs. 5(e) and 5(f), with varying positions of vertical slit shifts.

A 3D animation model containing a static five-star image background and a horizontal rotation object shown in Fig. 4 was used for hologram calculation as well. There are 180 frames of images and corresponding depth maps with a rotation angle of $-80°$ to $80°$. The model has a volume of 7.48 mm × 7.48 mm × 6 mm with 256 layers. The closest

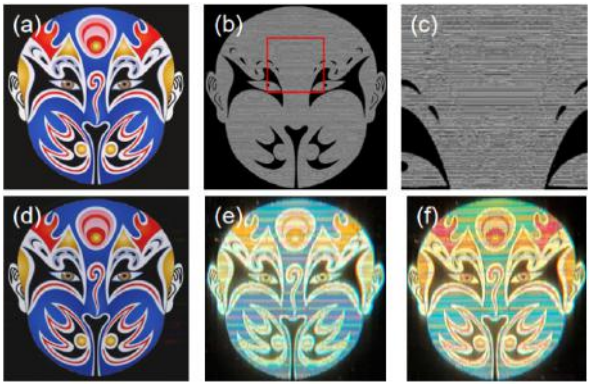

Fig. 5. (a) Target color object image, (b) calculated phase-only color rainbow hologram, (c) zoomed view of the red rectangle area in panel (b), (d) numerical reconstruction, (e) first optical reconstruction, and (f) second optical reconstruction.

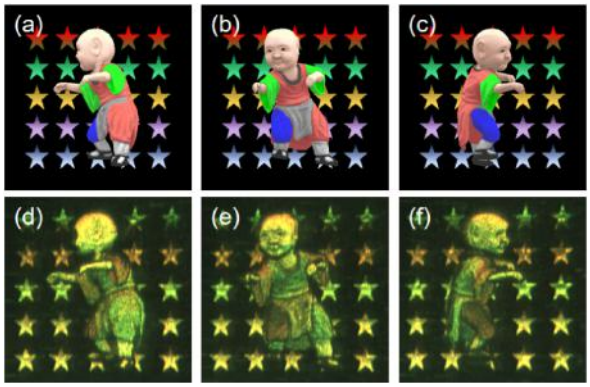

Fig. 6. Image frames of the 3D dynamic model: (a) first frame, (b) 80th frame, and (c) 160th frame. Reconstructed images from the corresponding phase full-color rainbow holograms with one slit position fixed: (d) first frame, (e) 80th frame, and (f) 160th frame. Visualization 1 shows the dynamic color 3D display result.

distance between the 3D object and the hologram plane was 4 mm. The optical reconstructions for some image frames are shown in Fig. 6. Visualization 1 is used to show the dynamic color 3D display result.

Since the holograms were illuminated by a white light source, we finally obtained narrow-band spectral components through the slit for the near-eye color display. The image color saturation is inevitably reduced, but we can obtain different color display effects by adjusting the slit position. In addition, the color of the reproduced images is related not only to the slit position but also to the spectral distribution of the illumination source. They can be optimized to improve the displayed colors. In our hologram calculation, the red, green, and blue images of the model are used directly without accurate color conversion for demonstration purposes. However, the color conversion discussed in Ref. [12] can be applied to improve the display results as well.

The total calculation time of a phase-only color rainbow hologram of the Beijing Opera facial makeup image is about 5.4 s in a MATLAB environment, where the calculation time of error diffusion is 4.9 s. It is feasible to increase the speed with graphics processing unit (GPU) acceleration for error diffusion and diffraction calculation [21].

In conclusion, we implement a phase-only color rainbow holographic near-eye display system in band-limited conditions by optimizing phase distributions in three primary color channels with the tailor-made bi-directional error diffusion algorithm and coding corresponding phase of reference waves. The full-color displays of the 2D image and the 3D dynamic color object have been successfully demonstrated, and both have the potential to be applied to head-mounted AR displays.

Funding. The National Natural Science Foundation of China (62005006).

Disclosures. The authors declare no conflicts of interest.

Data Availability. Data underlying the results presented in this Letter are not publicly available at this time but may be obtained from the authors upon reasonable request

REFERENCES

1. C. Chang, K. Bang, G. Wetzstein, B. Lee, and L. Gao, Optica **7**, 1563 (2020).
2. Y.-J. Wang, Y.-H. Lin, O. Cakmakci, and V. Reshetnyak, Opt. Express **28**, 23023 (2020).
3. D. Kim, S. Lee, S. Moon, J. Cho, Y. Jo, and B. Lee, Opt. Express **26**, 17170 (2018).
4. C. Jang, K. Bang, S. Moon, J. Kim, S. Lee, and B. Lee, ACM Trans. Graph. **36**, 1 (2017).
5. A. Maimone, A. Georgiou, and J. Kollin, ACM Trans. Graph. **36**, 1 (2017).
6. J. Jeong, J. Lee, C. Yoo, S. Moon, B. Lee, and B. Lee, Opt. Express **27**, 38006 (2019).
7. M.-H. Choi, Y.-G. Ju, and J.-H. Park, Opt. Express **28**, 533 (2020).
8. W. Lopes, L. Shi, F. Huang, W. Matusik, and D. Luebke, ACM Trans. Graph. **36**, 1 (2017).
9. Q. Gao, J. Liu, J. Han, and X. Li, Opt. Express **24**, 17372 (2016).
10. Z. Zhang, J. Liu, Q. Gao, X. Duan, and X. Shi, Opt. Express **27**, 7023 (2019).
11. J. C. Wyant, Opt. Lett. **1**, 130 (1997).
12. Y. Shi, H. Wang, Y. Li, H. Jin, and L. Ma, Appl. Opt. **48**, 4219 (2009).
13. T. Kozacki, M. Chlipala, and H.-G. Choo, Opt. Express **26**, 25086 (2018).
14. X. Yang, P. Song, H. Zhang, and Q.-H. Wang, Opt. Express **27**, 38236 (2019).
15. A. Jesacher, S. Bernet, and M. Ritsch-Marte, Opt. Express **22**, 17590 (2014).
16. H. Yoshikawa, T. Yamaguchi, and H. Uetake, Proc. SPIE **9771**, 97710N (2016).
17. T. Zhao and Y. Chi, Entropy **22**, 1354 (2020).
18. H. Song, G. Sung, S. Choi, K. Won, H.-S. Lee, and H. Kim, Opt. Express **20**, 29844 (2012).
19. P. W. M. Tsang and T.-C. Poon, Opt. Express **21**, 23680 (2013).
20. S. Jiao, D. Zhang, C. Zhang, and Y. Gao, T. Lei, and X. Yuan, IEEE J. Sel. Top. Quantum Electron. **26**, 2800108 (2020).
21. P. W. M. Tsang, A. S. M. Jiao, and T.-C. Poon, Opt. Express **22**, 5060 (2014).